Relationships between processing conditions, morphology, and I–V characteristics in P3HT:PCBM solar cells

M. Nasiri · F. Abbasi

Abstract In the present work, the effects of processing conditions comprising poly(3-hexylthiophene-2,5-diyl): [6,6]-phenyl-C_{61}-butyric acid methyl ester (P3HT:PCBM) ratio, P3HT concentration, co-solvent, thermal annealing, solvent annealing and the embedment of calcium as an exciton blocking layer on power conversion efficiency were studied. Polymer bulk heterojunction solar cells having a glass/ITO/PEDOT:PSS/P3HT:PCBM/(Ca)/Al sequence were fabricated. The main purpose of this work was to investigate the most effective parameters influencing the performance of polymer solar cells all in one study. Among these parameters, the role of high boiling point co-solvent such as N-Methyl-2-pyrrolidone, dimethyl sulfoxide and diiodooctane were emphasized. The morphology of the active layer was investigated using atomic force microscopy and field emission scanning electron microscopy (FESEM). The utilization of dimethyl sulfoxide as a co-solvent (5 %) led to larger heights on the surface whereas the solvent annealing reduced them and this sequence can disturb the size and distribution of PCBM domains. Incorporating diiodooctane as a co-solvent increased the short circuit current about three orders of magnitude. FESEM images showed a fibrillar structure for P3HT phase with approximately 25 nm in diameter and up to 250 nm in length. The presence of a thin Ca layer exhibited a significant effect on all I–V parameters, particularly on the fill factor.

M. Nasiri · F. Abbasi (✉)
Institute of Polymeric Materials, Sahand University of
Technology, Tabriz, Iran
e-mail: f.abbasi@sut.ac.ir

M. Nasiri · F. Abbasi
Faculty of Polymer Engineering, Sahand University of
Technology, Tabriz, Iran

1 Introduction

Research on organic photovoltaics is an interesting issue owing to some advantages including the utilization of simple and cost effective coating methods [1, 2], diversity of organic materials, transparency, flexibility, and so on. Due to low cost of polymer solar cells, they are good alternatives to traditional inorganic counterparts [3, 4]. The main disadvantage of the polymer solar cells is their low power conversion efficiencies (PCEs) [5, 6]. Since the discovery of electron transfer from conjugated polymer to buckminsterfullerene [7] and the introduction of the bulk heterojunction structures [8, 9], the power conversion efficiencies of polymer solar cells have been ascended by several orders of magnitude. Indeed, a realistic goal to achieve higher efficiencies rather than traditional inorganic solar cells is globally targeted. High absorption of polymer semiconductors [10], femto-second scale of charge transfer between polymer and fullerenes, and internal quantum efficiency for charge generation of the order of 0.95 [11] give this opportunity that by resolving the problem of charge collection, PCEs above 15 % will be achievable. The resistances of charge carriers transport through the active layer are related to the morphology of bulk heterojunction structure, and higher resistance provides more times for electrons and holes to recombine. Another important resistance is the barrier of charge transport between active layer and electrodes. For this reason, efforts have been devoted to manipulate the morphology of bulk heterojunction structure solar cells to achieve smaller transport resistances [12–14] using block copolymers [15], self-organization of polymer blends [16], processing additives [17], and side chain and pendent group manipulation [18, 19]. Also, other works were done to reduce the transport resistance in PEDOT:PSS layer using Ag nano

particles [20], dithienosilole copolymers [21], and organic salt in active layer [22]. However, less effort has been put to determine the relationships between the fabrication conditions, morphology of the active layer materials, and I–V characteristics of the solar cells. The need to have a deeper understand from these relationships in the P3HT:PCBM solar cells is both fundamental and practical. In this work, the polymer bulk heterojunction solar cells were fabricated and the morphology of the active layers was investigated using atomic force microscopy (AFM) and field emission scanning electron microscopy (FESEM). The main goal of this work was to investigate the effects of various processing conditions including P3HT:PCBM ratio, P3HT concentration, co-solvent, thermal annealing, solvent annealing and addition of calcium layer on the PCEs of the P3HT:PCBM solar cells. The effects of these parameters on the efficiency of solar cells are mainly discussed in terms of the morphological changes.

2 Experimental

2.1 Materials

Patterned indium tin oxide (ITO) coated substrates was purchased from Ossila Corp. with a sheet resistance of 20 $\Omega/\square$ and 150 nm in thickness. Poly(3,4-ethylenedioxythiophene):poly(styrenesulfonate) (PEDOT:PSS), P3HT (4002-EE), [60] PCBM (99 %), o-dichlorobenzene (o-DCB) and 1,8-diiodoocatane were prepared from Sigma aldrich, Rieke Metals Inc., Solenne Inc., Merck, and Alfa Aesar, respectively. All materials were used as received.

2.2 Measurements and instruments

The active layer morphology and its thickness were studied using a DualScope^{TM} DS-95-50E/Rasterscope C26 atomic force microscope (AFM). The thicknesses of PEDOT:PSS and active layers was measured by Dektak profilometer. FESEM images were taken by Tescan model MIRA3 FEG-SEM and analyzed by image J software. I–V characteristic of the fabricated solar cells were measured by IVIUM CompactStat under the illumination of AM1.5G, 100 mW cm^{-2} using Luzchem Photoreactor Model LZC-SSR solar simulator. The calibration was done using a Thorlab calibrated photodiode. Each solar cell contained six pixels which were evaluated separately, and the reported I–V parameters of each sample were the average of them.

2.3 Fabrication of polymer solar cells

After 10 min sonication of substrates in 10 % NaOH aqueous solution, the protective layers of ITO coated substrates were detached and removed by tweezers. For further cleaning, the substrates were twice sonicated in 5 % KOH aqueous solution for 5 min. The procedure was continued by rinsing twice with distilled water and sonication in isopropyl alcohol for 5 min. The substrates were dried with nitrogen gun and exposed to UV-O$_3$ for 20 min. PEDOT:PSS dispersion was filtered by a 0.45 μm PTFE membrane, and spin coated on clean ITO coated glass at 2,000 rpm for 2 min. The thickness of this layer was about 50 nm. The cathode strip was cleaned with moisturized cotton bud and heated at 125 °C for 15 min in a nitrogen glove box.

P3HT was dissolved in o-DCB by mixing at 50 °C for 2 h followed by mixing at room temperature for 12 h. After addition of specific amount of PCBM, the solution was mixed for 12 h at room temperature. Additives were added 1 h before coating. After filtering with a 0.45 μm PTFE membrane, the solution was spin coated on PEDOT:PSS layer during 90 s and stored in an open Petri dish in the glove box. Solvent annealing was performed in a small Petri dish by addition of 100 μl of o-DCB or bromobenzene (BB). Samples were placed in a mask and put into a thermal evaporator. Ca and Al were deposited at about 5×10^{-6} mbar in a one-step evacuation. Thermal annealing was done on a hot plate at 125 °C for 30 min. The solar cells were encapsulated by applying one drop of UV-curable epoxy resin and placing a glass on them. The samples were stored under UV exposure for 20 min.

3 Results and discussion

To investigate the effect of P3HT:PCBM ratio on PCE of the fabricated solar cells, this value was chosen in the range of 1:0.77–1:3. As shown in Fig. 1, by increasing the P3HT:PCBM ratio from 1:0.77 to 1:1 the short circuit current density (I$_{SC}$) increased from 0.715 to 1.72 mA/cm^2. By further increasing the P3HT:PCBM ratio, it decreased
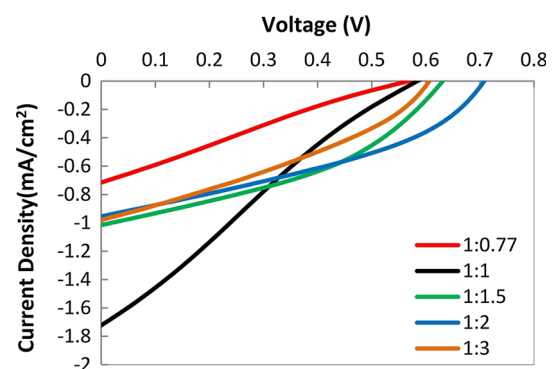

Fig. 1 I–V characteristics at different P3HT:PCBM ratios for the devices with a Ca layer (samples no. 14, 15, 16, 17, 18)

to 1 mA/cm^2. The open circuit voltage (V$_{OC}$) increased to about 0.7 V at the ratio of 1:2 and then decreased to 0.6 V at the ratio of 1:3. The increase of V$_{OC}$ to 0.7 V can be attributed to good contact between P3HT and PCBM phases. Maximum fill factor (FF) (40 %) was obtained at 1:1.5 ratio. Although the best power conversion efficiency (PCE) was obtained for 1:1.5 ratio, it seems that the 1:2 ratio having a higher V$_{OC}$ and a FF value comparable with the FF value corresponding to 1:1.5 ratio, is an optimum ratio.
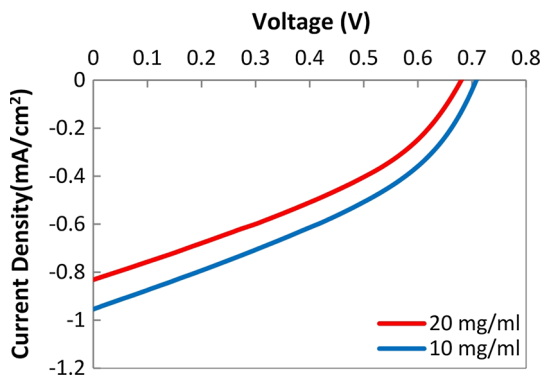
Fig. 2 I–V characteristics at different P3HT concentrations for devices over coated with a Ca layer (samples no. 12, 17)
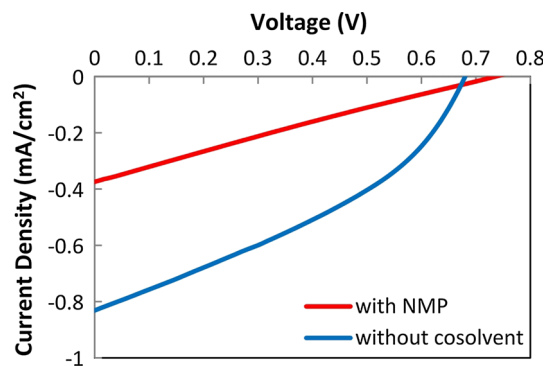

Fig. 5 The effect of NMP treatment on the I–V characteristics of devices having a Ca layer (samples no. 12, 13)
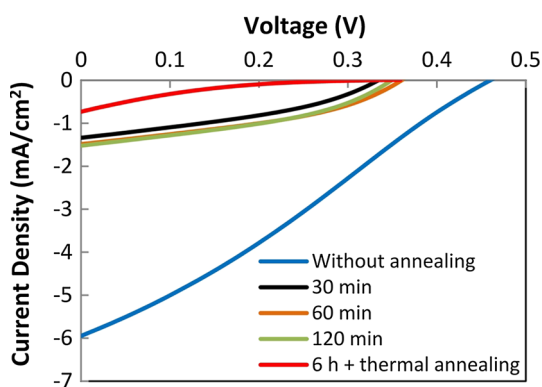

Fig. 3 Thermal and solvent annealing effects on the I–V characteristics for devices with diiodooctane and without a Ca layer (samples no. 4, 7, 8, 9, 3)
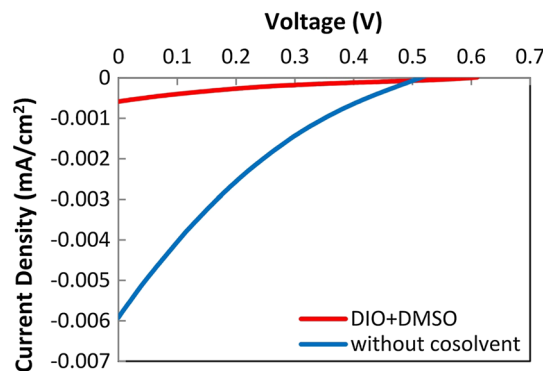

Fig. 6 The effects of diiodooctane and DMSO as co-solvents on the I–V characteristics for devices fabricated without a Ca layer (samples no. 1, 2)
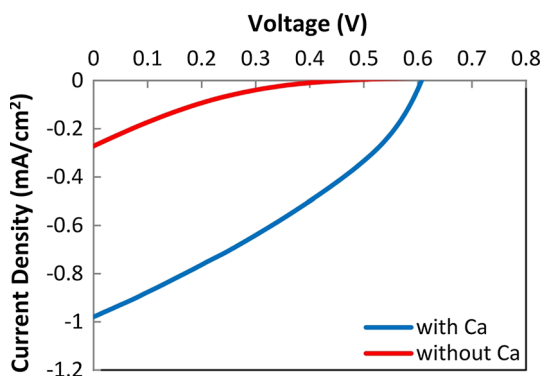

Fig. 4 The effect of Ca layer as an exciton blocking layer on the I–V characteristics for devices fabricated without diiodooctane and annealing process (samples no. 11, 18)
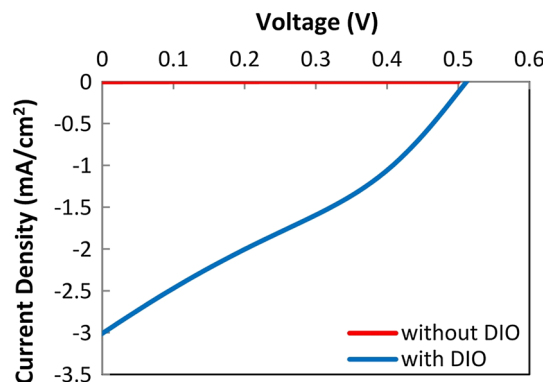

Fig. 7 The effect of diiodooctane on the I–V characteristics for devices fabricated without a Ca layer (samples no. 10, 5)

The effect of P3HT concentration on the I–V characteristics of devices with a same P3HT:PCBM ratio (1:2) and consisting of an over coated Ca layer was evaluated (Fig. 2). By decreasing the P3HT concentration V_{OC}, I_{SC} and FF were on the rise from 0.679, 0.832 and 36.6 to
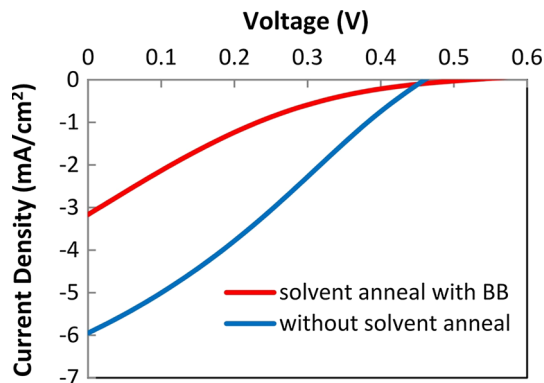

Fig. 8 The effect of solvent annealing with bromobenzene on the I–V characteristics (samples no. 4, 19)
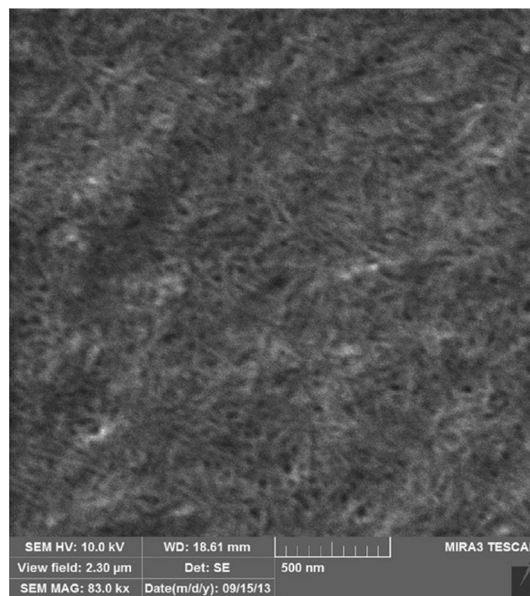

Fig. 9 FESEM image taken from surface of the sample with 1:2 P3HT:PCBM ratio, 20 mg/ml P3HT concentration and 5 v % diiodooctane

Table 1 The processing conditions and I–V characteristic of the samples

Sample	P3HT:PCBM	C_{P3HT} (mg/ml)	Co-solvent	Thermal anneal	Solvent anneal	Ca thickness (nm)	I_{SC} (mA/cm^2)	V_{OC} (V)	FF (%)	PCE (%)
1	1:1	20	–	125	–	0	0.0059	0.510	17.0	0.0005
2	1:1	13.3	DIO[a] + DMSO[b]	125	–	0	6E−04	0.6	15.4	5E−05
3	1:2	20	DIO	125	6 h	0	0.738	0.324	13.4	0.0320
4	1:2	20	DIO	–	–	0	5.95	0.460	28.2	0.772
5	1:2	10	DIO	125	6 h	0	3.02	0.509	31.4	0.482
6	1:3	20	DIO	–	–	0	5.66	0.36	23.2	0.473
7	1:2	20	DIO	–	0.5 h	0	1.34	0.33	37.2	0.164
8	1:2	20	DIO	–	1 h	0	1.49	0.36	39.0	0.209
9	1:2	20	DIO	–	2 h	0	1.52	0.345	39.7	0.208
10	1:2	10	–	125	0.5 h	0	0.0024	0.440	10.1	0.0001
11	1:2.9	14.6	–	–	–	0	0.272	0.455	15.8	0.0195
12	1:2	20	–	–	–	26.9	0.832	0.679	36.6	0.206
13	1:2	20	NMP[c]	–	–	26.9	0.374	0.734	23.7	0.065
14	1:0.77	10	–	–	–	15	0.715	0.565	23.7	0.095
15	1:1	10	–	–	–	15	1.72	0.584	23.8	0.239
16	1:1.5	10	–	–	–	15	1.02	0.63	40.0	0.255
17	1:2	10	–	–	–	15	0.954	0.705	37.9	0.254
18	1:3	10	–	–	–	15	0.979	0.605	33.9	0.200
19	1:2	20	DIO	–	4 min, BB[d]	26.9	3.17	0.52	15.3	0.25

[a] Diiodooctane

[b] Dimethysulfoxide

[c] N-methylpyrrolidone

[d] Bromobenzene

0.705, 0.954 and 37.9 %, respectively. As a result, PCE increased from 0.206 to 0.254 %. Decline of the active layer solution concentration reduces the active layer thickness, and leads to a better mixing of P3HT and PCBM phases during film formation. Although a thinner active layer has a smaller photon absorption, thicker one causes a bigger series resistance which can lower all the I–V characteristics. The similar shapes of the diagrams confirm that

Fig. 10 FESEM image taken from cross section of the sample with 1:2 P3HT:PCBM ratio, 20 mg/ml P3HT concentration and 5 v % diiodooctane

the observed effect is related to the thickness of the active layer.

Regarding Fig. 3, solvent annealing reduces the V_{OC} and I_{SC} by inducing large PCBM domains, which could be observed visually, but increases the FF probably by easing the extraction of accumulated charges near the cathode electrode. After 6 h solvent annealing and subsequent thermal annealing at 125 °C, I_{SC} and FF decrease from 5.95 and 28.2 to 0.738 and 13.4 %, respectively.

The existence of a Ca layer as an exciton blocking layer improves the I–V characteristic of the solar cells (Fig. 4), in particular the FF which increased from 15.8 to 33.9 %.

The effect of addition of *N*-methyl-2-pyrrolidone (NMP) (Fig. 5), diiodooctane and DMSO (Figs. 6, 7) was also investigated. Respecting Fig. 5, addition of 5 v % NMP can improve the V_{OC} of the cell, probably by improving the P3HT and PCBM interfacial contact, but reduces the I_{SC} and FF. The latter is ascribed to non optimized phase sizes developed by NMP treatment. The results of this experiment show that a high V_{OC} (0.734 V) is achievable in P3HT:PCBM solar cells. The existence of diiodooctane can increase I_{SC} by three orders of magnitude. The addition of 5 % DMSO to the solution containing 5 % diiodooctane significantly lowered the PCE by formation of micron-size mountains. Solvent annealing by bromobenzene (Fig. 8) for 4 min reduces the I_{SC}, FF and PCE from 5.95, 28.2 and 0.772 to 3.17, 15.3 and 0.25 %, respectively, and increases the V_{OC} value from 0.46 to 0.52. This increase is probably due to the insertion of Ca layer. Details of processing conditions and measured I–V characteristics of the all experiments are presented in Table 1.
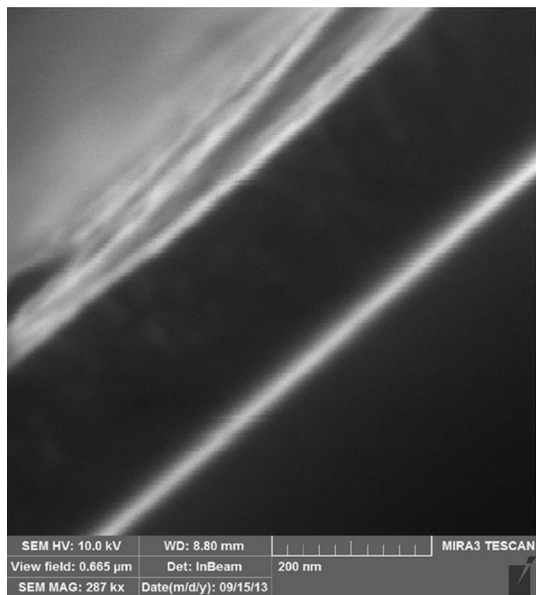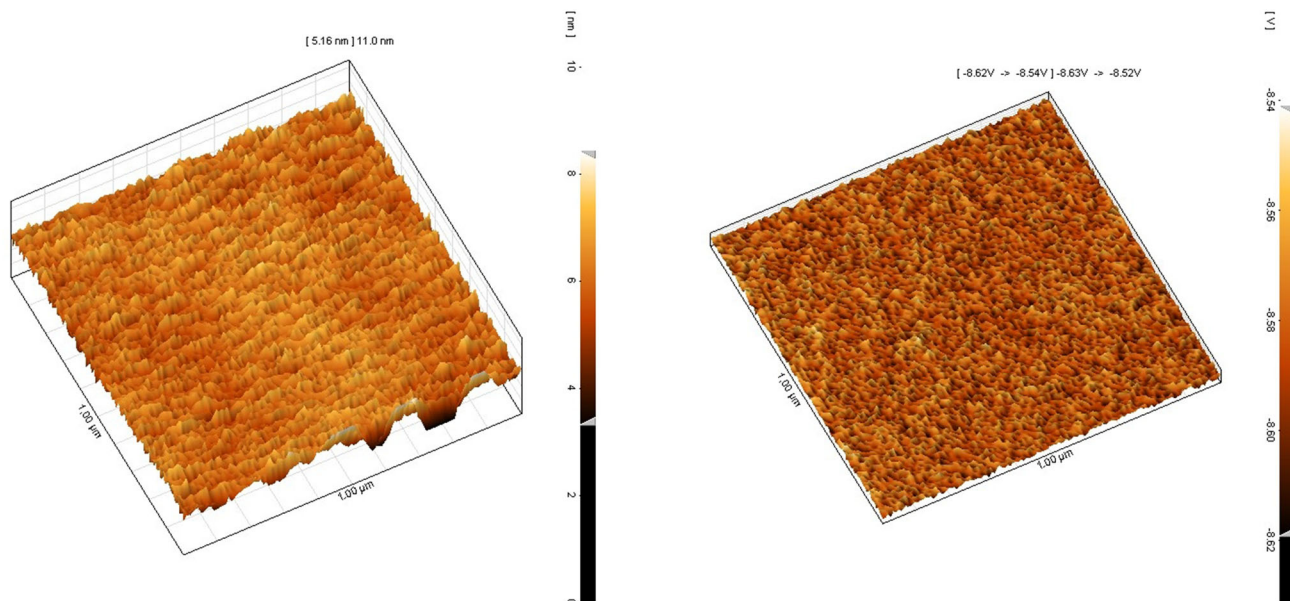

Fig. 11 AFM topography (*left*) and phase (*right*) images of a sample with P3HT:PCBM ratio of 1:2, 20 mg/ml P3HT concentration, and without diiodooctane and any annealing process (no. 12)
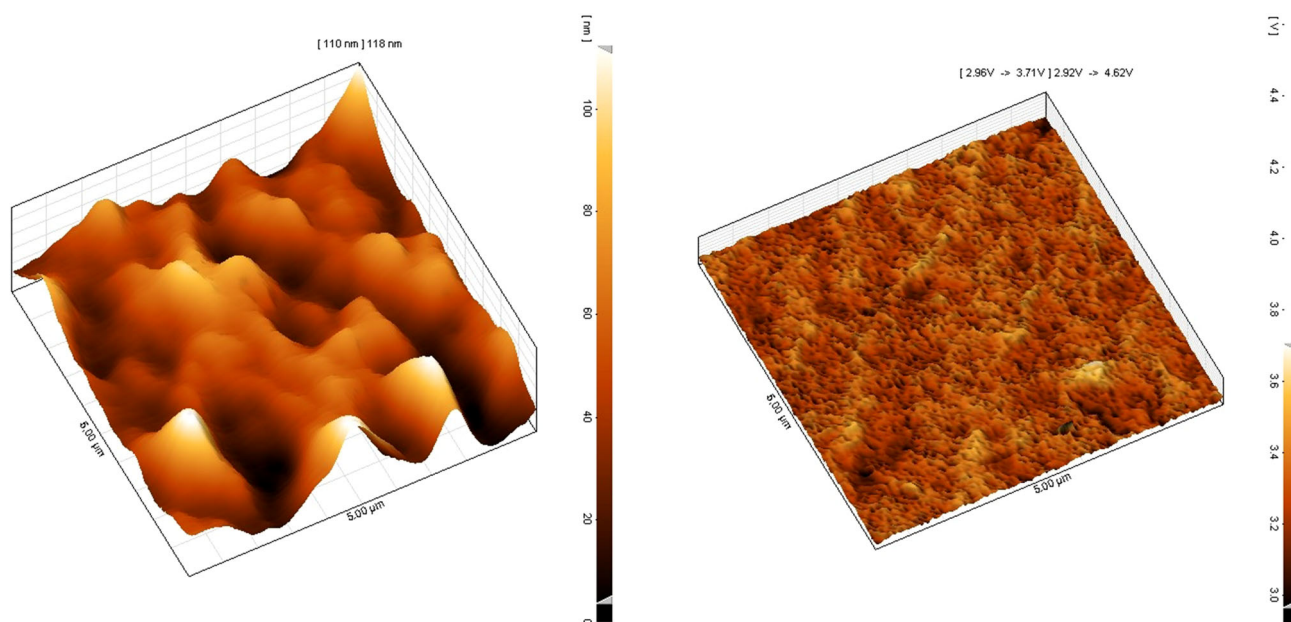
Fig. 12 AFM images a sample with 1:2 P3HT:PCBM ratio, 20 mg/ml P3HT concentration, 5 v % diiodooctane, and without any annealing process (sample no. 4)
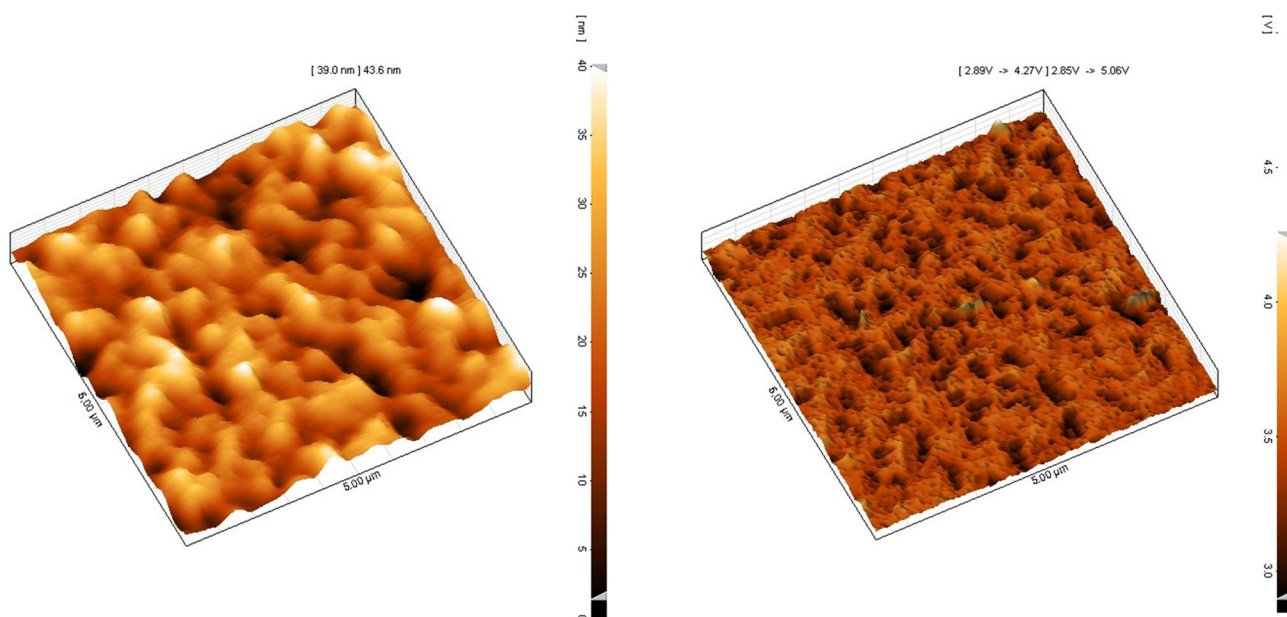

Fig. 13 AFM images of a sample with 1:2 P3HT:PCBM ratio, 20 mg/ml P3HT concentration, 5 v % diiodooctane. Solvent annealing was carried out with bromobenzene for 4 min (sample no. 19)

The FESEM micrograph obtained from the surface of a P3HT:[60]PCBM film (Fig. 9) confirms that the P3HT chains are regulated in a fibrillar structure with around 25 nm in diameter and up to 250 nm in length. These fibrils are oriented in the horizontal plane via spin coating process. If these fibrils were oriented in the vertical direction, the hole mobility would increase drastically. The FESEM image obtained from the cross section of a P3HT:[60]PCBM (1:2)

film and treated with 5 % diiodooctane as a co-solvent (Fig. 10) depicts that the size of PCBM grains is approximately 27 nm. The exciton diffusion length in P3HT is <8.5 nm [23–25]. Hence, it is expected that by further reducing the PCBM domain sizes and consequent reduction of their distances, the current density increases.

AFM topography and phase images of the sample with P3HT:PCBM ratio of 1:2 and without any additive are
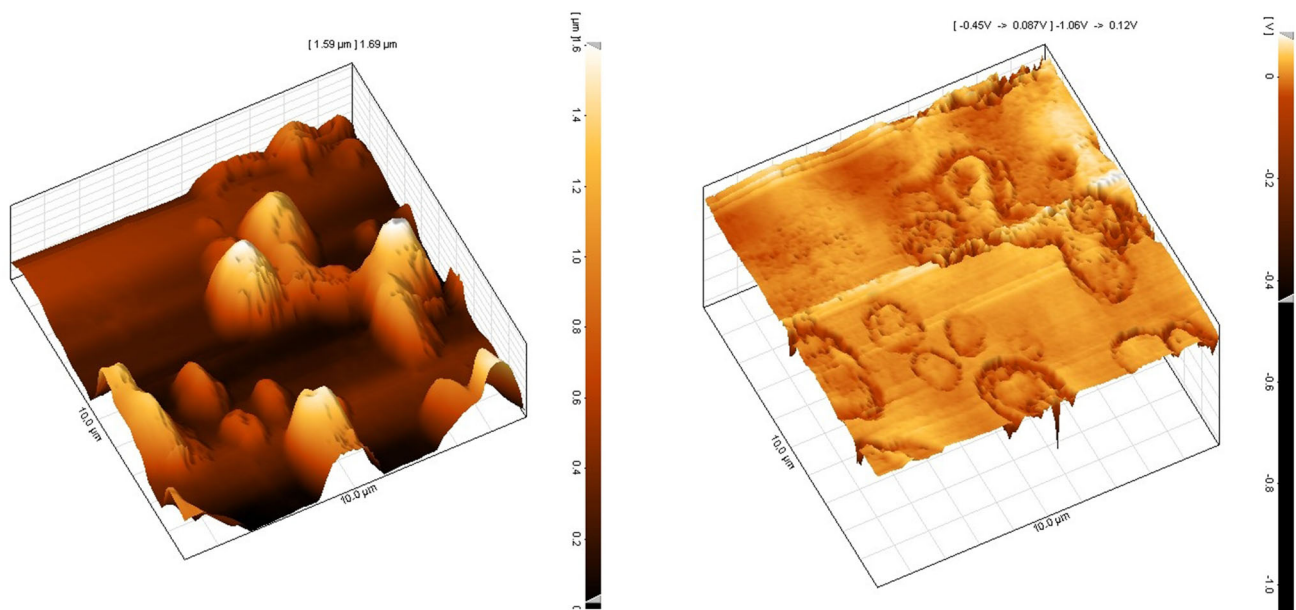
Fig. 14 AFM images of a sample with 1:1 P3HT:PCBM ratio, 13.3 mg/ml P3HT concentration, 5 v % diiodooctane and 5v % DMSO. Thermal annealing was carried out at 125 °C (sample no. 2)
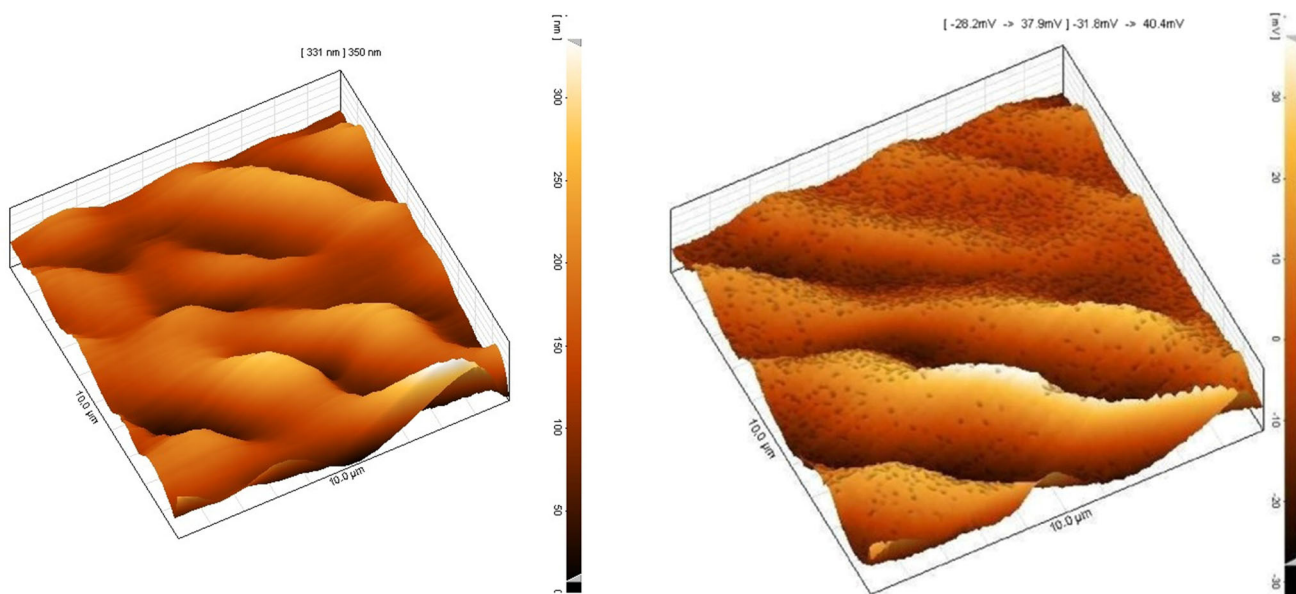

Fig. 15 AFM images of a sample with 1:1 P3HT:PCBM ratio, 13.3 mg/ml P3HT concentration, 5 v % diiodooctane and 5v % DMSO. Thermal annealing and solvent annealing were carried out at 125 °C and 8 h, respectively

illustrated in Fig. 11. The most probable height at 1 μm scale is 6 nm and maximum height is 11 nm. The PCBM domains are uniformly distributed and their average size is about 30 nm. Incorporating 5 v % diiodooctane into the P3HT:PCBM solution resulted in a rougher surface with 45 nm of most probable height and 118 nm of maximum height (Fig. 12). The majority of PCBM domains grew up to 80 nm; however, the larger domains were also produced in the range of 250 nm. By solvent annealing with

bromobenzene for 4 min (Fig. 13), distinct larger domains were produced, and surface went smoother with most probable height of 22 nm and maximum height equal to 44.7 nm. The growth of PCBM domains continued and large domains outgrew up to 700 nm, but the size of most domains remained at 80 nm.

Figure 14 indicates that by addition of 5 % diiodooctane and 5 % DMSO into the P3HT:PCBM solution, discrete micron-size mountains are produced and the majority of

Table 2 Quantitative data of obtained from AFM analyses

Sample No.	Maximum height (nm)	Most probable height (nm)	Root mean square deviation (nm)
12	11.0	6	0.621
4	118	45	19.4
2	1,690	250	325
2 + Solvent annealing	350	130	50.6
19	44.7	22	6.57

PCBM phase is located around the edges of these mountains. While solvent annealing with o-DCB washed the discrete mountains into small channels (Fig. 15), the size of PCBM domains remained approximately constant. On the other hand, these domains were washed into the valleys (dark regions in phase image). Therefore, the mean distance between PCBM domains at mountains was of the order of micrometer which resulted in very low power conversion efficiencies. Quantitative data of topographic images are represented in Table 2.

4 Conclusions

In this study, the P3HT:[60]PCBM based polymer solar cells were fabricated and the effects of P3HT:[60]PCBM ratio, P3HT concentration, co-solvent, thermal annealing, solvent annealing and calcium exciton blocking layer on PCE were studied. AFM analyses demonstrated that while solvent annealing with *o*-DCB washes the discrete mountains into small channels, the size of PCBM domains remains approximately constant. The PCBM domains were washed into the valleys and the mean distance between PCBM domains at mountains was of the order of micrometer resulting in very low power conversion efficiencies. When the pristine roughness of the surface was in a nano scale this phenomena did not occur. AFM topography image of the sample with P3HT:PCBM ratio of 1:2 and without any additive was very smooth, whereas by incorporating 5 % diiodooctane a rougher surface was

obtained, and the size of most of the PCBM domains grew up. The FESEM image of the surface of P3HT:[60]PCBM confirmed that the P3HT chains were regulated in a fibrillar structure. The FESEM image of the cross section of P3HT:[60]PCBM (1:2) with 5 % diiodooctane, as a co-solvent, showed the size of PCBM grains were approximately 35 nm. It is expected by further reducing the PCBM domains size and better distribution of them, the higher current density will be acquired.

References

1. Y. Xia, R.H. Friend, Macromolecules **38**, 6466 (2005)
2. F.C. Krebs, S.A. Gevorgyan, J. Alstrup, J. Mater. Chem. **19**, 5442 (2009)
3. C.J. Brabec, N.S. Sariciftci, J.C. Hummelen, Adv. Funct. Mater. **11**, 15 (2001)
4. C.J. Brabec, Sol Energy Mater Sol C **83**, 273 (2004)
5. F. Padinger, R.S. Rittberger, N.S. Sariciftci, Adv. Funct. Mater. **13**, 1 (2003)
6. S.E. Shaheen et al., Appl. Phys. Lett. **78**, 841 (2001)
7. N.S. Sariciftci et al., Science **258**, 1474 (1992)
8. G. Yu et al., Science **270**, 1789 (1995)
9. H. Hoppe, N.S. Sariciftci, Adv. Polym. Sci. **214**, 1 (2008)
10. A.C. Arango et al., Adv. Mater. **12**, 1689 (2000)
11. J. Piris et al., J. Phys. Chem. C **113**, 14500 (2009)
12. A.J. Moul, K. Meerholz, Adv. Mater. **20**, 240 (2008)
13. C.J. Brabec et al., Adv. Mater. **22**, 3839 (2010)
14. H. Hoppe, N.S. Sariciftci, J. Mater. Chem. **16**, 45 (2006)
15. J.A. Gratt, R.E. Cohen, J. Appl. Polym. Sci. **91**, 3362 (2004)
16. G. Li et al., Nature Mater **4**, 864 (2005)
17. J.K. Lee et al., J. Am. Chem. Soc. **130**, 3619 (2008)
18. W. Li et al., Polymer **51**, 3031 (2010)
19. Q. Hou et al., J. Mater. Sci.: Mater. Electron. **24**, 4284 (2013)
20. X. Li et al., J. Mater. Sci.: Mater. Electron. **25**, 140 (2014)
21. Q. Hou et al., J. Mater. Sci.: Mater. Electron. **24**, 536 (2013)
22. N.S. Sabri et al., J. Mater. Sci.: Mater. Electron. **24**, 2183 (2013)
23. P.E. Shaw, A. Ruseckas, I.D.W. Samuel, Adv. Mater. **20**, 3516 (2008)
24. H. Wang et al., Nanoscale **3**, 2280 (2011)
25. M.C. Heiber, A. Dhinojwala, J. Phys. Chem. C **117**, 21627 (2013)